Award Number: W81XWH-14-1-0056

TITLE:
Tumor Tension Induces Persistent Inflammation and Promotes Breast Cancer Aggression

PRINCIPAL INVESTIGATOR: Ori Maller

CONTRACTING ORGANIZATION:
University of California, San Francisco
San Francisco CA 94103-4249

REPORT DATE: October 2015

TYPE OF REPORT: Annual

PREPARED FOR: U.S. Army Medical Research and Materiel Command
Fort Detrick, Maryland 21702-5012

REPORT DOCUMENTATION PAGE

Form Approved
OMB No. 0704-0188

1. REPORT DATE *(DD-MM-YYYY)*	**2. REPORT TYPE**	**3. DATES COVERED** *(From - To)*
October 2015	Annual	09-30-2014 to 09-29-2015

4. TITLE AND SUBTITLE

Tumor Tension Induces Persistent Inflammation and Promotes Breast Cancer Aggression

5a. CONTRACT NUMBER
W81XWH-14-1-0056

5b. GRANT NUMBER

5c. PROGRAM ELEMENT NUMBER

6. AUTHOR(S)

Ori Maller and Valerie M. Weaver
email: ori.maller@ucsfmedctr.org

5d. PROJECT NUMBER

5e. TASK NUMBER

5f. WORK UNIT NUMBER

7. PERFORMING ORGANIZATION NAME(S) AND ADDRESS(ES)

University of California, San Francisco
1855 Folsom St STE 425
San Francisco CA 94103-4249

8. PERFORMING ORGANIZATION REPORT NUMBER

9. SPONSORING / MONITORING AGENCY NAME(S) AND ADDRESS(ES)

U.S. Army Medical Research and
Materiel Command
Fort Detrick, Maryland 21702-5012

10. SPONSOR/MONITOR'S ACRONYM(S)

11. SPONSOR/MONITOR'S REPORT NUMBER(S)

12. DISTRIBUTION / AVAILABILITY STATEMENT

Approved for Public Release; Distribution Unlimited

13. SUPPLEMENTARY NOTES

14. ABSTRACT

Human breast tumors are highly fibrotic and their ECMs are stiffer relative to benign lesions. More recently, we established positive correlations between the number and location of infiltrating immune cells and ECM stiffness in human breast tumors. This has led us to hypothesize that TAMs drive tissue fibrosis and subsequently may stimulate inflammatory signaling. Using the MMTV-PyMT model, early macrophage not only ablated lung metastases, but demonstrated an anti-fibrotic role for macrophages as depicted by a decrease in fibrillar collagen and a reduction in ECM stiffness. Interestingly, we observed a striking loss of phospho-STAT3 and FAK signaling when mice were treated with a CSF1 antagonist. Furthermore, when mice were treated with a LOX inhibitor, phospho-STAT3 levels decreased in tumor cells. We also found that LOX inhibitor treatment caused a shift in the cytokine milieu consistent with an anti-tumor immune response. Moreover, tumor cells that lacked STAT3 manifest an analogous trend in cytokine milieu in vivo. Lastly, we demonstrated that ECM stiffness increased in phospho-STAT3 in tumor cells in vitro. Collectively, our data suggest macrophage infiltration promotes fibrosis that stimulates inflammatory signaling in tumor cells during early mammary tumorigenesis — and this feed-forward loop induces a pro-tumor immune response.

15. SUBJECT TERMS

16. SECURITY CLASSIFICATION OF:			**17. LIMITATION OF ABSTRACT**	**18. NUMBER OF PAGES**	**19a. NAME OF RESPONSIBLE PERSON**
a. REPORT	**b. ABSTRACT**	**c. THIS PAGE**			USAMRMC
Unclassified	Unclassified	Unclassified	Unclassified	35	**19b. TELEPHONE NUMBER** *(include area code)*

Table of Contents

Introduction:

Human breast tumors are highly fibrotic and their extracellular matrices (ECMs) are stiffer relative to benign lesions. A major contributor to tumor mechanics is fibrillar collagen-rich ECM. During tumor progression, fibrillar collagen content increases and its organization is characterized by bundles of aligned collagen fibers that are oriented perpendicular, particularly on the invasive fronts in both mouse models of breast cancer and human disease. We demonstrated that a stiffened ECM and elevated mechanosignaling (e.g. β1 integrin-focal adhesion kinase signaling axis) promoted mammary tumorigenesis, whereas reducing ECM stiffening impeded tumor formation. More recently, we observed significant correlations between macrophage infiltration and ECM stiffness in luminal B and basal-like breast cancer, but not luminal A. My original hypothesis was that tumor cell tension and ECM stiffening cooperate with inflammatory signaling to facilitate immune evasion and promote breast cancer aggression. In this progress report, I present our latest data that led us to generate a refined hypothesis: macrophages promote fibrosis during early tumorigenesis that induces inflammatory signaling, resulting in a feed-forward loop to induce immune suppresion and subsequently breast cancer aggression.

Keywords:

BAPN	beta-aminoproprionitrile
CSF	Colony stimulating factor
ECM	Extracellular matrix
FAK	Focal adhesion kinase
ITGB1	Integrin β1
IL	Interleukin
PyMT	Polyoma virus- middle T antigen
LOX	Lysyl Oxisdase
LuBC	Luminal breast cancer
qPCR	Quantitative polymerase chain reaction
STAT3	Signal transducer and activator of transcription 3
TAM	Tumor-associated macrophages
TGFβ	Transforming growth factor β
TIC	Tumor-initiating cells
TNBC	Triple-negative breast cancer
TuDC	Tumor-associated dendritic cells

Accomplishments/Changes/Problems:

After careful consideration, we agree with Reviewer A that we must have a better understanding of our models — and especially the temporal relationship between fibrotic reaction and immune response. In fact, our hypothesis evolved due to the striking observation tumor-associated macrophages (TAMs) has a pro-fibrotic role when mice were treated colony-stimulating factor 1 antagonist (anti-CSF1 antibody) during early tumorigenesis resulted in a decrease in fibrillar collagen and a reduction in ECM stiffness (Figure 1A-B). Interestingly, I also observed a loss of phospho-STAT3 and FAK signaling when macrophages were depleted (Figure 2A) and we detected diminished metastatic incidence, which we used as a readout of tumor aggression (Figure 2B). In accordance with the macrophage depletion data, STAT3 phosphorylation levels in tumor cells decreased in mammary tumors when mice were treated with a LOX inhibitor (Figure 3A). Moreover, we demonstrated that ECM stiffness directly increased STAT3 phosphorylation in tumor cells *in vitro* by using collagen I-coated polyacrylamide gels (Figure 3B); further, this increase in phospho-STAT3 was impeded with FAK inhibitor (Figure 3B). Moreover, ECM adjacent to mammary tumor cells that lacked STAT3 was softer and a quantitative cytokine profile of these tumors revealed a shift toward an anti-tumor immune response (see Aim 2 for data).

Altogether, we provide multiple lines of evidence in this progress report to argue that macrophage infiltration promotes fibrosis in early tumorigenesis and subsequently stimulates inflammatory signaling in tumor cells — and this feed-forward loop induces a pro-tumor immune response. These findings emphasize the significance

of temporal regulation by macrophages and potentially a distinct role in fibrosis and immune evasion. To further address this notion, we are prepared to perform RNA-seq on TAMs to assess pro-fibrotic and immune-related pathways at two different time points; this experiment should address whether TAMs with the same cell surface markers alter their function during tumor progression in the PyMT model.

This related work is critical to establish a temporal understanding of our *in vivo* models and help to better design an efficacious treatment plan, when we would combine anti-fibrotic agent and immunotherapy. I will further discuss below our progress on each Specific Aim.

Specific Aim 1: Examine if β1 integrin–mediated tumor cell tension increases the levels of inflammatory cytokines and degree of immunosuppression in LuBC and TNBC mouse models.

Task 1A. Generate the appropriate breeding scheme to build cohorts of tri-transgenic mice (*MMTV-PyMT; MMTV-Cre; LSL-Itgb1$^{V737N/+}$* mice and *C3(1)/Tag; MMTV-Cre; LSL-Itgb1$^{V737N/+}$* mice). The control for these studies will be *MMTV-PyMT* or *C3(1)/Tag; LSL-Itgb1$^{V737N/+}$* mice. I will start by breeding with hemizygous *MMTV-Cre; LSL- LSL-Itgb1$^{V737N/+}$* male mice with hemizygous *LSL- LSL-Itgb1$^{V737N/+}$* female mice to generate *MMTV-Cre; LSL-Itgb1$^{V737N/V737N}$* female or male mice. Then I will cross these mice with hemizygous *MMTV-PyMT* or *C3(1)/Tag* mice in the corresponding gender. These breeding scheme should result in ~12.5% female me as *MMTV-PyMT* or *C3(1)/Tag; MMTV-Cre; LSL-Itgb1$^{V737N/+}$* female mice depending on the breeding and another ~12.5% as control. *(Month 3-7)*

I will need a total of 20 mice for each group per model to obtain statistical power of at least a two-fold reduction in tumor growth (assuming large standard deviation).

Task 1B. Monitor tumor growth and animal health for *MMTV-PyMT; MMTV-Cre; LSL-Itgb1$^{V737N/+}$* and control mice. FAK inhibitor treatment will begin prior to the presence of palpable tumors. *(Month 7-11)*

Task 1C. Monitor tumor growth and animal health for *C3(1)/Tag; MMTV-Cre;; LSL-Itgb1$^{V737N/+}$* mice. FAK inhibitor treatment will begin prior to the presence of palpable tumors. *(Month 7-15)*

Task 1D. Flow cytometry analyses will be performed at study endpoints using 13 different markers to characterize the immune cell profile as described in the project narrative. *(Months 11 and 15)*

Task 1E. Inflammatory cytokine analyses will be performed at study endpoints. *(Months 11 and 15)*

Task 1F. OCT-embedded and frozen mammary tumors from Task 1B and C will be used to quantify collagen deposition and organization via second harmonic generation (SHG) analysis and picro sirius red (PS) staining. Stromal stiffness will be measured using nanoindentation Atomic Force Microscopy (AFM). *(Months 11-15 for Task 1B and 15-19 for Task 1C)*

Task 1G. Immunofluorescence analyses will be done using marker for Mechanosignaling and inflammatory pathways as described in the project narrative. *(Months 11-15 for Task 1B and 15-19 for Task 1C)*

Task 1H. I will seek assistance from a trained pathologist to review histological sections to determine tumor grade and invasiveness. *(Months 11-15 for Task 1B and 15-19 for Task 1C)*

Progress on Aim 1:

Task 1A-C:
We received in the past year two novel transgenic mouse models — and we have already started the validation process or are in the final breeding stages. The first model is an inducible lysyl oxidase (LOX), which was validated by: 1) detecting GFP in epithelial cells using MMTV-rtTA; TetO_mLOX mdoel (Figure 4A); and 2) assessing collagen crosslinking, fibrillar collagen I deposition, and macrophage infiltration in a pilot study using MMTV-PyMT;Col1a1-tTA;TetO_mLOX model, where LOX was overexpressed in Col1a1+ activated fibroblasts (Figure 4B-C). The second model is an inducible LOX knockout model: MMTV-PyMT;Col1a1-CreERT;$LOX^{flx/flx}$; although the initial validation has been done with MMTV-Cre *in vivo* or Adenovirus-Cre *in vitro* (Figure 5C-D). We decided to center our effort on these models for the following reasons: 1) to address reviewers concerns and pursue transgenic mouse models, where tumor stroma is being altered by lysyl oxidase induction in activated fibroblasts; and 2) these approaches would allow us to directly alter ECM crosslinking and stiffness.

However, we decided to generate a C3(1)/TAg; MMTV-Cre; LSL-$Itgb1^{V737N/\ V737N}$ female mice due to data obtained in Aim 3.

Task 1D:
I performed an extensive flow cytometry analyses on MMTV-PyMT or C3(1)/TAg mice treated with BAPN — a LOX inhibitor — to gauge on the role of collagen crosslinking and ECM stiffness on immune cell composition. Unfortunately, the impact of BAPN treatment was unremarkable on either T cell or myeloid cell composition in MMTV-PyMT model (Figure 6 & 7). Nevertheless, I also sorted TAMs and we are planning to perform RNA-seq because tumors could contain the same number of TAMs, but these cells may have a distinct function depending on treatment. Of note, a caveat of this experiment is that we don't fully understand the off target effects of BAPN, especially on fast-growing tumors like MMTV-PyMT; our new transgenic models would address this concern. Nevertheless I observed a trend toward an increase in CD8+ T cell/ T-Reg cell ratio in the BAPN group compared with control in C3(1)/TAg model (Figure 8A-B), but not MMTV-PyMT model; these data suggest ECM crosslinking may contribute to a more productive cytotoxic CD8 T cell function in basal-like breast cancer model.

Task 1E:
Our collaborator performed a preliminary cytokine array on MMTV-PyMT tumors, where they found a significant decrease IL6 and TNFα, and a trend toward an increase in IFNγ in tumors from mice treated with BAPN compared with control (Figure 9A). Of note, we are going to evaluate additional cytokines in order to better match our data in Aim 2. In addition, through our collaboration with Kirk Hansen, we also found that arginine levels are increased in tumors from mice treated with BAPN (Figure 9B), which further suggests a shift toward anti-tumor immune response. We have recently obtained enough tumors from this mouse model to perform a more extensive cytokine analysis. It would be informative to compare the changes between this model and the inducible LOX mouse model as BAPN is currently heavily used to alter collagen crosslinking by many researchers who study fibrosis and tumor microenvironment.

Task 1F:
We have already published that BAPN treatment alters ECM stiffness, collagen deposition and organization in MMTV-PyMT tumors. In addition, I found BAPN significantly reduces ECM stiffness and for a lesser degree collagen deposition in C3(1)/TAg tumors (see Aim 3).

Task 1G:
In progress

Task 1H:
In progress

Specific Aim 2: Determine whether constitutively active STAT3 in mammary tumor cells increases invasiveness by promoting immune evasion, enhancing cellular contractility and ECM stiffness.

Task 2A. Generate the appropriate breeding scheme to build cohorts of tri-transgenic mice (*MMTV-PyMT; Stat3$^{C/+}$* mice and *C3(1)/Tag; Stat3$^{C/+}$* mice). The control for these studies will be *MMTV-PyMT* or *C3(1)/Tag; Stat3$^{+/+}$* mice. I can try to generate homozygous *Stat3$^{C/C}$* mice; however these mice die within 4 months. These breeding scheme should result in ~12.5% female me as *MMTV-PyMT* or *C3(1)/Tag; Stat3$^{C/+}$* female mice depending on the breeding and another ~12.5% as control. *(Month 7-11)*

I will need a total of 20 mice for each group per model to obtain statistical power of at least a two-fold reduction in tumor growth (assuming large standard deviation).

Task 2B. Monitor tumor growth and animal health for *MMTV-PyMT; Stat3$^{C/+}$* and control mice. FAK inhibitor treatment will begin prior to the presence of palpable tumors. *(Month 11-15)*

Task 2C. Monitor tumor growth and animal health for *C3(1)/Tag; Stat3$^{C/+}$* mice. The β-aminopropionitrile inhibitor treatment will begin prior to the presence of palpable tumors. *(Month 11-19)*

Task 2D. Same as Task 1D. *(Months 15 and 19)*

Task 2E. Inflammatory cytokine analyses will be performed at study endpoints. *(Months 15 and 19)*

Task 2F. Same as Task 1F. *(Months 15-19 for Task 2B and 19-23 for Task 2C)*

Task 2G. Same as Task 1G. *(Months 15-19 for Task 2B and 19-23 for Task 2C)*

Task 2H. Same as Task 1H. *(Months 15-19 for Task 2B and 19-23 for Task 2C)*

Task 2I. Proposed *in vitro* studies will be completed as described in the project narrative. *(Months 15-23)*

Progress on Aim 2:

Task 2A:
We decided to work with the conditional STAT3 knockout model because it would be difficult to discern the function of each cellular compartment in the constitutively active STAT3 model, where all tumor, stromal, and immune cells have higher levels of STAT3 activity. We focus on STAT3 activity in epithelial cells becasue: 1) we aim to understand how tumor cells and tissue mechanics influence cytokine milieu; 2) a role for STAT3 activity in tumor-initiating cells (TICs) is established in mouse models of breast cancer; and 3) we have evidence that there is a direct correlation between TIC expansion (CD24 high CD29 pos) and alterations in immune cell composition consistent with pro-tumor immune response during mammary tumor progression (Figure 10-11).

I completed multiple studies with *MMTV-PyMT; MMTV-Cre; Stat3$^{flx/flx}$* to assess the effects of epithelial STAT3 on cytokine milieu and fibrosis in mammary tumors. Consistently with previously published data, we observed a significant decrease in metastatic incidence in the STAT3 KO group compared with control (Figure 12A-B).

Task 2B-C:
Completed for MMTV-PyMT model. I found no difference in tumor growth when STAT3 knocked out in epithelial cells (data not shown). I didn't perform any studies yet looking on the effects of FAK inhibitor or BAPN treatment.

Task 2D:
In progress

Task 2E:
Completed for MMTV-PyMT model. I found a shift in cytokine milieu in whole mammary tissue homogenates from STAT3 KO mice compared with control consistent with anti-tumor immune response (Figure 12C).

Task 2F:
Completed for MMTV-PyMT model. I found a decrease in ECM stiffness and fibrillar collagen deposition in the STAT3 KO group compared with control (Figure 13A-B).

Task 2G:
In progress. I observed a decrease in phospho-SMAD2 Ser465/Ser467 in stromal cells adjacent to MMTV-PyMT tumors in mice, where STAT3 was knocked out in epithelial cells (Figure 13C). This is consistent with our data showing a decrease in ECM stiffness and a reduction in TGFβ levels in the STAT3 KO group in mice. Thus, I am currently evaluating impact of TGFβ and ECM stiffness on macrophage polarization using co-culture models.

Task 2H:
In progress

Specific Aim 3: Test if anti-fibrotic treatment reduces mechanosignaling and STAT3 activity, while potentiating the effects of immunotherapy to impede metastatic disease.

Task 3A. I will treat C3(1)/Tag mice and MMTV-PyMT with low dosage simvastatin starting at 2 months and 4 weeks, respectively. Spontaneous tumor models are more similar to the human condition and allow us to better assess how treatment influences immunity and disease progression. *(Months 3-10)*

I will need a total of 10 mice for each group per model to assess whether simvastatin induces changes in tumor immunity and tissue tension.

In addition, if needed, I will inject tumor cell lines using an orthotopic syngeneic model. This approach will allow us to take a mechanistic approach and determine functions of specific signaling modulators (STAT3 or β1 integrin mutant). This approach will involve isolating mammary tumor cells from C3(1)/Tag and MMTV-PyMT mouse model. I will prepare several cell lines where I manipulate β1 integrin and/or STAT3. I will generate derivative 4 cell lines for each original cell line (MMTV-PyMT (obtained from Dr. Werb's lab, UCSF) and C3(1)/Tag): 1) β1 integrin mutant overexpression and STAT3 knockdown; 2) Constitutively active STAT3 overexpression and β1 integrin knockdown; 3) β1 integrin mutant and constitutively active STAT3 overexpression; 4) β1 integrin mutant and constitutively active STAT3 knockdown. Inject tumor cell lines into the 4^{th} mammary gland and monitor tumor growth and metastatic incidence. *(Months 10-15)*

I will need a total of 5-10 mice for each group per model to assess whether a specific signaling modulator induces changes in tumor immunity and tissue tension. If variations within specific groups will be greater than expected, I may need to increase the number of animals.

Task 3B. Same as Task 1D.

Task 3C. Same as Task 1E.

Task 3D. Same as Task 1F.

Task 3E. Same as Task 1G.

Task 3F. Monitor tumor cell invasion and contractility in collagen gels in the presence of simvastatin using the tumor cell lines described in Task 3A. *(Months 5-7)*

Task 3G. Same as Task 1A if I decided to use transgenic mouse model (1st choice). Otherwise, I will use orthotopic model using tumor cell lines generated in 3A. *(Months 23-31)*

Task 3H. Monitor tumor growth and animal health. Simvastatin treatment will start prior to the presence of palpable tumors. Short-term treatment with chemotherapeutic (alone) or immunotherapeutic agent (in combination with simvastatin) will be initiated when control mice are expected to have malignant disease.

I will need a total of 20 mice for each group per model to obtain statistical power of at least a two-fold reduction in tumor growth (assuming large standard deviation).

Task 3I. Same as Task 1D.

Task 3K. Same as Task 1E.

Task 3L. Same as Task 1F.

Task 3M. Same as Task 1G.

Progress on Aim 3:

Task 3A:
In progress. I isolated primary mammary tumor cells from C3(1)/TAg model; however, these cell lines didn't form tumors when injected to syngeneic FVB/n strain female mice. I will need to further different component in medium and characterize the isolated cells to make sure I don't select for a subpopulation of tumor cells with low tumorigenicity. In the meantime, I decide to focus on testing the effects of simvastatin treatment on tumors in the C3(1)/TAg model (transgenic, not orthotopic). I am also at the final stages of obtaining several breeding pairs for: C3(1)/TAg; MMTV-Cre; LSL-Itgb1$^{V737N/\ V737N}$ mice.

Task 3B:
In progress. I isolated primary tumor organoids from C3(1)/TAg model and embedded in collagen I gels. The primary tumor organoids didn't adapt to these collagen gels as the PyMT organoids using the same defined media. We are trying to figure out these cell culture issues with isolated cells from C3(1)/TAg model.

Task 3C-E:
In progress. Interestingly, I found that mammary tumors in C3(1)/TAg are more fibrotic and have higher number of αSMA+ cancer-associated fibroblasts compared with MMTV-PyMT (Figure 14) — similar to work we have recently published, where basal-like tumors are more fibrotic relative to luminal B. To begin addressing the effect of simvastatin on tissue fibrosis in mammary tumorigenesis, I treated mice with BAPN, low or high dosage of simvastatin in C3(1)/TAg model — I determined clinically-relevant dosages of simvastatin by using FDA-recommended conversion factor from human to mice. I observed significantly smaller tumors in mice treated with high dose of simvastatin compared to control (Figure 15B). Moreover, high dose simvastatin treatment decreased levels of phospho-FAK Y397 and ECM stiffness (Figure 15C), but quantitative analyses would be necessary to determine differences in fibrillar collagen deposition and aSMA fibroblasts. This reduction in mechanosignaling significantly correlated with a decrease in ECM stiffness (Figure 15D).

Once we have enough breeding pairs, I will use C3(1)/TAg; MMTV-Cre; LSL-Itgb1$^{V737N/\ V737N}$ mice to determine if enhanced integrin signaling in tumor cells increases metastatic incidence as it is usually very low in C3(1)/TAg (only ~10% of mice). I will also have an arm with high dose simvastatin treatment.

Task 3F:
In progress.

Task 3G-K:

I identified a meaningful increase in CD103+ DC — this population is known to be a potent inducer of CD8+ T cell activity — in mammary tumors of mice treated with high dose of simvastatin (Figure 16A-B); however, such an increase was not observed with mice treated with BAPN due high variance among tumors in this group. We suspect that the simvastatin impedes tumor cell contractility as suggested by the phospho-FAK Y397 staining — and it induces changes in ECM stiffness and possibly cytokine milieu. To test this hypothesis, we are generating C3(1)/TAg; MMTV-Cre; LSL-Itgb1$^{V737N/\ V737N}$ model and I will proceed with these tasks in this model. Of note, in future experiment, we will use a myeloid panel that would better discern among myeloid population similar to figure 6.

Figure legends:

Figure 1: Early macrophage depletion attenuates fibrosis and ECM stiffness in mammary tumors. MMTV-PyMT female mice were treated with IgG control or anti-CSF1-neutralizing antibody i.p. delivered starting at 4 weeks of age. Mice were euthanized at 11 weeks of age.
(A) Fibrillar collagen architecture and deposition were assessed via 2-photon/ second harmonic generation imaging and picrosirus red staining. N=5-6 mice per group.
(B) ECM stiffness adjacent to MMTV-PyMT tumors has been evaluated via atomic force microscopy (AFM). N=4-5 mice per group and at least two force maps per sample. Statistical analysis performed using unpaired Student's t-test.
(C) Schematic of our putative model.

Figure 2: Early macrophage depletion decreases STAT3 phosphorylation in epithelial cells.
(A) Representative images of F4/80 TAM, phospho-FAK Y397, and phospho-STAT3 staining in mammary tumors from MMTV-PyMT tumors from 11-week-old female mice via immunofluorescence (IF); DAPI was used for nuclear staining. Scale bars, 100µm. N=5-6 mice per group.
(B) Lung metastases were detected using quantitative PCR (qPCR) on RNA from whole-tissue homogenates. Statistical analysis performed using unpaired two-tailed Student's t-test.

Figure 3: Stiffer ECM promotes STAT3 phosphorylation in mammary tumor cells *in vivo* and in vitro.
(A) Representative images of phospho-STAT3 Y705 and activated β1 integrin staining via IF in MMTV-PyMT tumors from 11-week-old female mice. Scale bars, 100µm. N=5 mice per group.
(B) Representative images of STAT3 pY705 was evaluated in mammary tumor cell line (MET1) when cultured on polyacrylamide gels in various stiffness levels via immunoblotting. We used 1µM PND-1186 to inhibit FAK activity.
(C) Schematic of our putative model.

Figure 4: Proof-of-concept experiment to validate tet-inducible lysyl oxidase transgenic mouse.
(A) MMTV-rtTA; TetO_mLOX mice have been treated with 2 mg/mL DOX plus 5% sucrose starting 6 weeks of age. Tumor cells were isolated and analyzed using flow cytometry.
(B) MMTV-PyMT;Col1a1-tTA;TetO_mLOX mice have been taken off DOX treatment at 6 weeks of age. Collagen crosslinking has been determined on mammary tumors from 11-week-old MMTV-PyMT mice by mass spectrometry. N=3-4 mice per group. *p>0.05 by one-tailed Student's t-test. LOX OX= lysyl oxidase overexpression.
(C) Fibrillar collagen architecture and deposition were assessed via picrosirus red staining. F4/80 TAM and pan-cytokeratin were examined via IF. N=3-4 mice per group.

Figure 5: Proof-of-concept experiment to validate LOX knockout model.
(A) Genomic DNA has been isolated from control ($LOX^{flx/flx}$) and MMTV-Cre; $LOX^{flx/flx}$ showing proper excision LOX exon 2 *in vivo*.
(B) Mouse mammary epithelial cells were isolated from mice with the floxed LOX allele. These cells were treated with adeno-cre to elicit genomic recombination of exon 2 *in vitro*. RNA was isolated from these cells to establish attenuated expression of the LOX enzyme upon recombination. Of note, expression levels were not completely gone likely due to the heterogeneous Cre recombination.

Figure 6: BAPN treatment didn't alter myeloid cell composition in MMTV-PyMT tumors.
Immune cell composition was assessed in 11-week-old mice via flow cytometry. N=5-6 per group.

Figure 7: BAPN treatment didn't alter T cell composition in MMTV-PyMT tumors.
Immune cell composition was assessed in 11-week-old mice via flow cytometry. N=4-6 per group.

Figure 8: Simvastatin treatment enhances CD103+ dendritic cell infiltration and thus may elicit to anti-tumor immune response

(A) Flow cytometric data of dendritic cell (DC) populations found in C3(1)/TAg tumors. The data are representative of 4 to 6 mice per group.

(B) Plots depict percent positive CD11c+CD206 low DCs or CD103+ CD11b low DCs out of total CD45+ cells from tumors treated with BAPN or simvastatin. Statistical analysis performed using unpaired Student's t-test assess the relationship between control group and high-dose simvastatin group.

Figure 9: BAPN treatment impedes pro-tumor immune response in MMTV-PyMT model.

(A) ELISA-based assay determined cytokine levels in MMTV-PyMT tumors. N=9 mice.

(B) Arginine levels were detected in whole-tissue homogenates in 11-week-old mice via mass spectrometry.

Figure 10: Tumor-initiating cell population expends during tumor progression.

TIC profile on mammary tissues from MMTV-PyMT model from 8-week-old and 11-week-old mice was performed using multicolor flow cytometry. This relationship is significant, *p>0.05 by unpaired two-tailed Student's t-test.

Figure 11: A shift in the type of macrophages correlates with the transition from a premalignant lesion to mammary carcinoma.

Immune cell profile on mammary tissues from MMTV-PyMT model from 8-week-old and 11-week-old mice was performed using multicolor flow cytometry. All relationships are significant, *p>0.05 by unpaired two-tailed Student's t-test.

Figure 12: Knocking out STAT3 in epithelial cells shift cytokine milieu toward anti-tumor immunity.

(A) STAT3 pY705 was evaluated in tumors from MMTV-PyMT mice to confirm STAT3 knockout in epithelial cells via IF.

(B) Lung metastases were detected using qPCR on RNA from whole-tissue homogenates. Statistical analysis performed using unpaired two-tailed Student's t-test.

(C) Quantitative immunoassay was used to examine cytokine levels in tumors. All relationships are significant, *p>0.05 by unpaired two-tailed Student's t-test.

Figure 13: Epithelial STAT3 increases tissue fibrosis and ECM stiffness as well as stromal TGFβ-SMAD2 signaling in mammary tumors

(A) Fibrillar collagen architecture and deposition were assessed via 2-photon/ second harmonic generation imaging. N=4-5 mice per group

(B) ECM stiffness adjacent to MMTV-PyMT tumors has been evaluated via AFM. N=4-5 mice per group and at least two force maps per sample. Statistical analysis performed using unpaired two-tailed Student's t-test.

(C) Representative images of cytokeratin and phospho-SMAD2 Ser465/467 staining in mammary tumors from MMTV-PyMT tumors from 11-week-old female mice via IF. N=6 mice per group.

(D) Schematic of our putative model.

Figure 14: C3(1)/Tag — mouse model of basal-like breast cancer— is significantly more fibrotic than MMTV-PyMT.

Representative images of picro-sirus red and αSMA staining. Scale bars, 100μm

Figure 15: High-dosage of simvastatin treatment hampers tumor growth rate and reduces FAK phosphorylation

(A) Schematic of study design.

(B) Tumors were measured bi-weekly and growth rates were calculated by fitting a straight line among measurements. N=7 mice. Statistical analysis performed using one-way ANOVA with Kruskal-Wallis test to

assess overall significance (*p<0.05) and an unpaired Student's t-test to assess the relationship between control group and high-dose simvastatin group.
(C) Representative images of picro-sirus red, αSMA and phosphor-FAK Y397 staining. Scale bars, 100µm.
(D) ECM stiffness adjacent to C3(1)/TAg tumors has been evaluated via AFM. N=7 mice per group and at least two force maps per sample. Statistical analysis performed using unpaired two-tailed Student's t-test.

Figure 16: Simvastatin treatment enhances CD103+ dendritic cell infiltration and thus may contribute to anti-tumor immune response
(A) Flow cytometric data of dendritic cell (DC) populations found in C3(1)/TAg tumors. The data are representative of 4 to 6 mice per group.
(B) Plots depict percent positive CD11c+CD206 low DCs or CD103+ CD11b low DCs out of total CD45+ cells from tumors treated with LOX inhibitor (BAPN) or simvastatin.

Figure 1

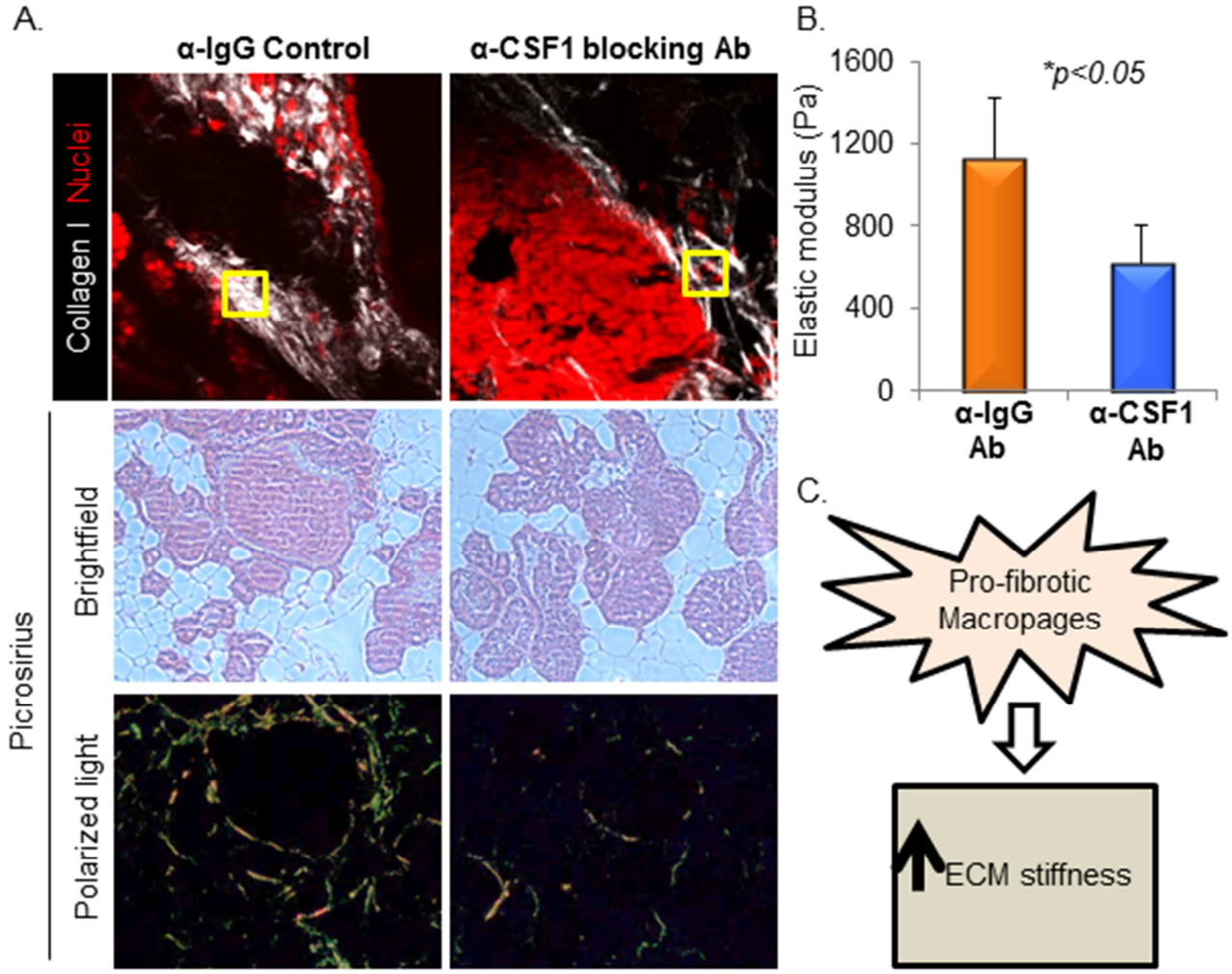
A.
α-IgG Control
α-CSF1 blocking Ab
Collagen I Nuclei
Picrosirius
Brightfield
Polarized light
B.
*p<0.05
Elastic modulus (Pa)
1600
1200
800
400
0
α-IgG Ab
α-CSF1 Ab
C.
Pro-fibrotic Macropages
ECM stiffness

Figure 2

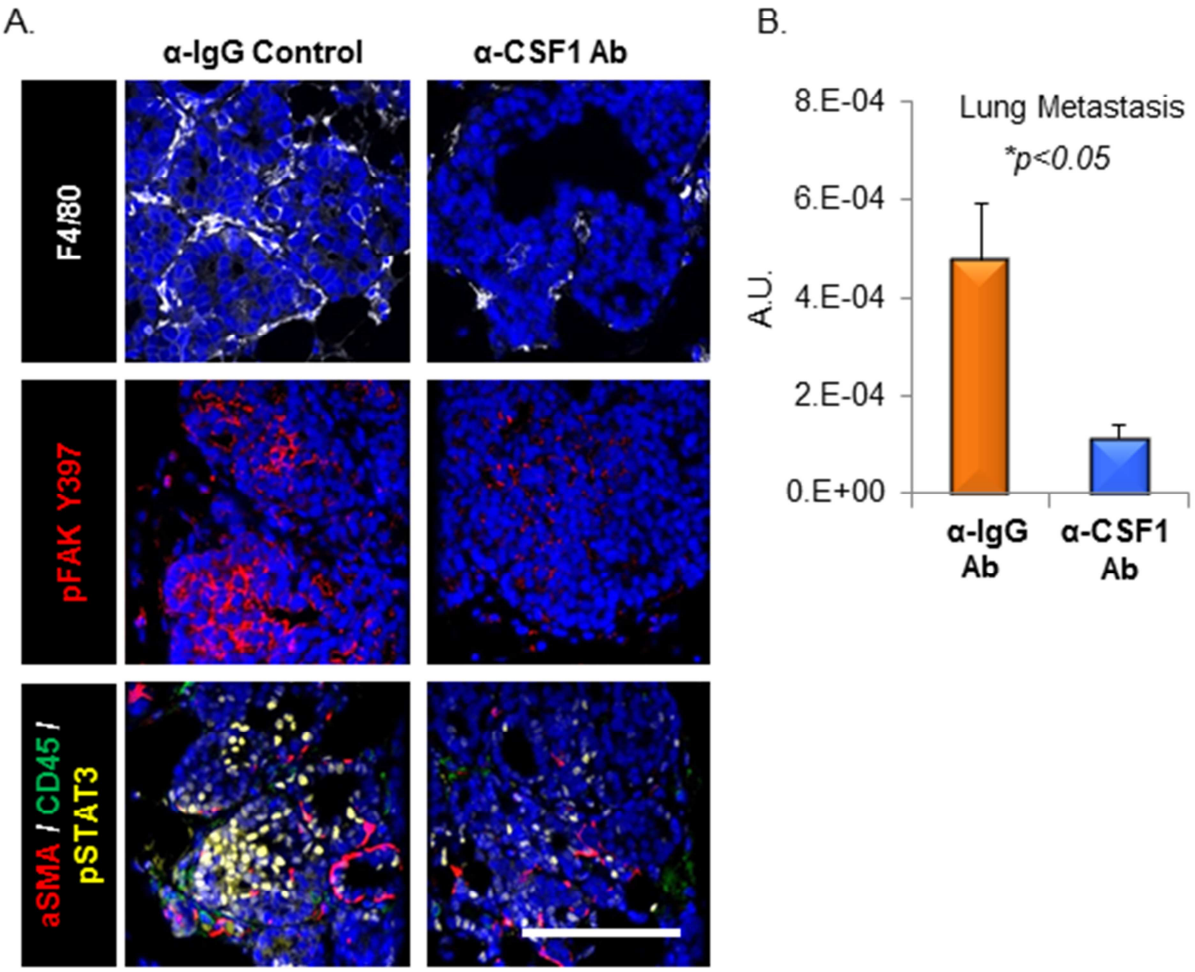
A.
α-IgG Control
α-CSF1 Ab
F4/80
pFAK Y397
aSMA / CD45 / pSTAT3
B.
Lung Metastasis
*p<0.05
A.U.
8.E-04
6.E-04
4.E-04
2.E-04
0.E+00
α-IgG Ab
α-CSF1 Ab

Figure 3

A.

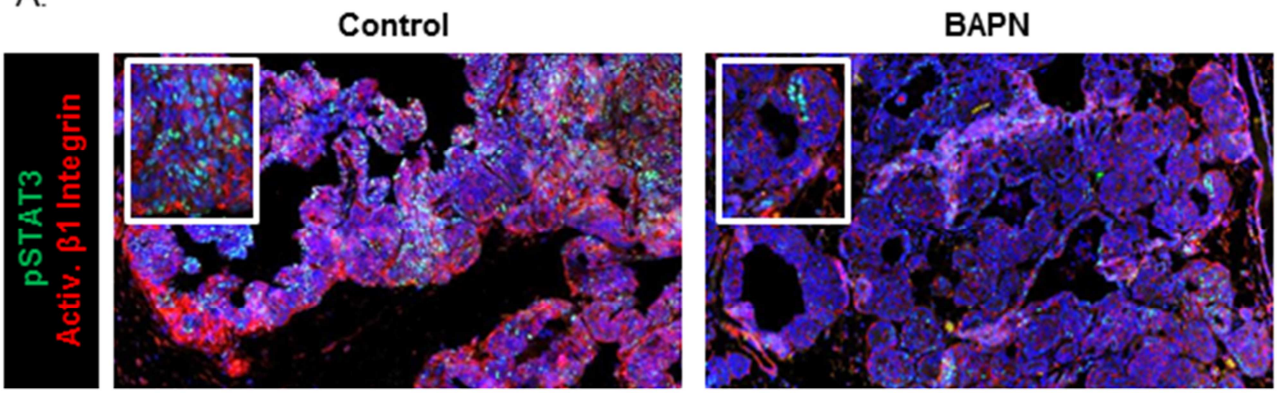
Control
BAPN
pSTAT3
Activ. β1 Integrin

B.

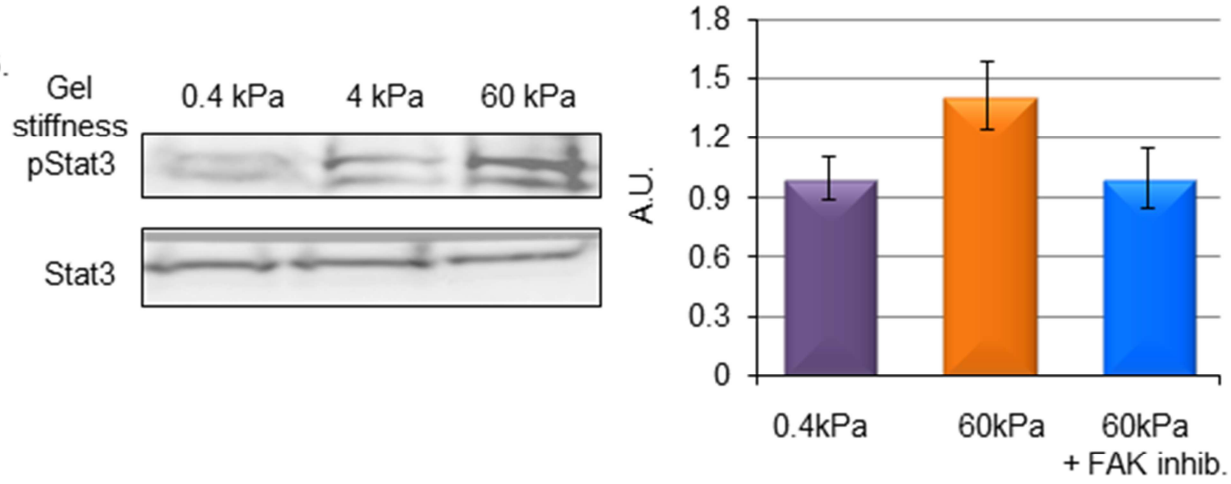
Gel stiffness
0.4 kPa
4 kPa
60 kPa
pStat3
Stat3
A.U.
1.8
1.5
1.2
0.9
0.6
0.3
0
0.4kPa
60kPa
60kPa + FAK inhib.

C.

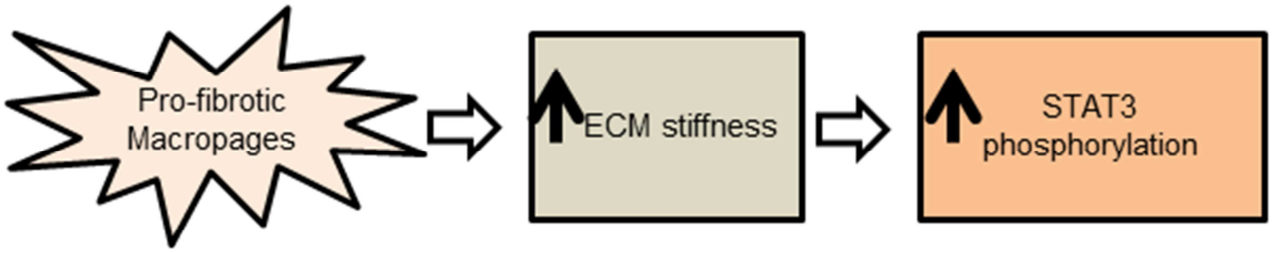
Pro-fibrotic Macropages
ECM stiffness
STAT3 phosphorylation

Figure 4

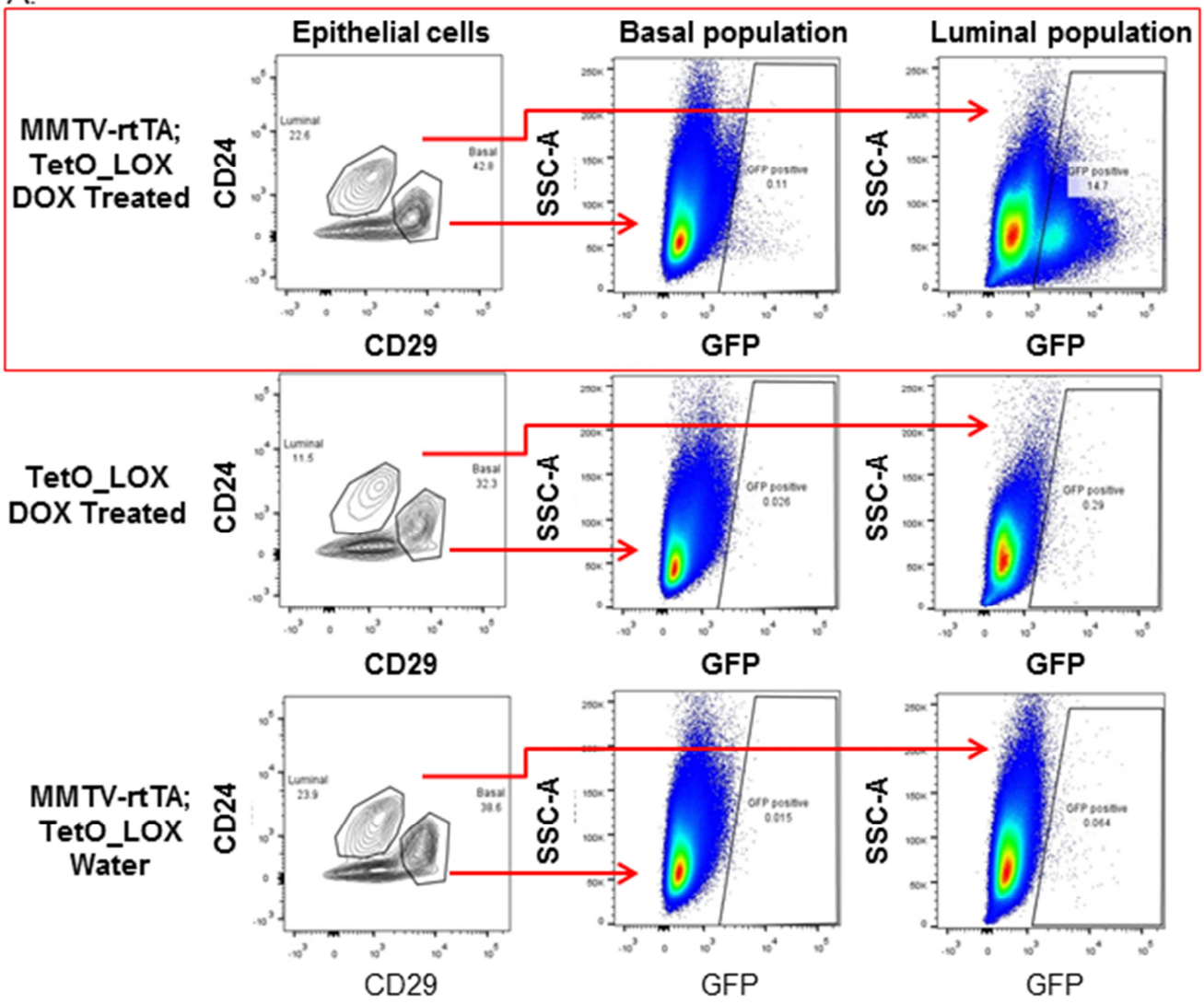
A.
Epithelial cells
Basal population
Luminal population
MMTV-rtTA; TetO_LOX DOX Treated
TetO_LOX DOX Treated
MMTV-rtTA; TetO_LOX Water
CD24
CD29
SSC-A
GFP
Luminal
Basal
GFP positive

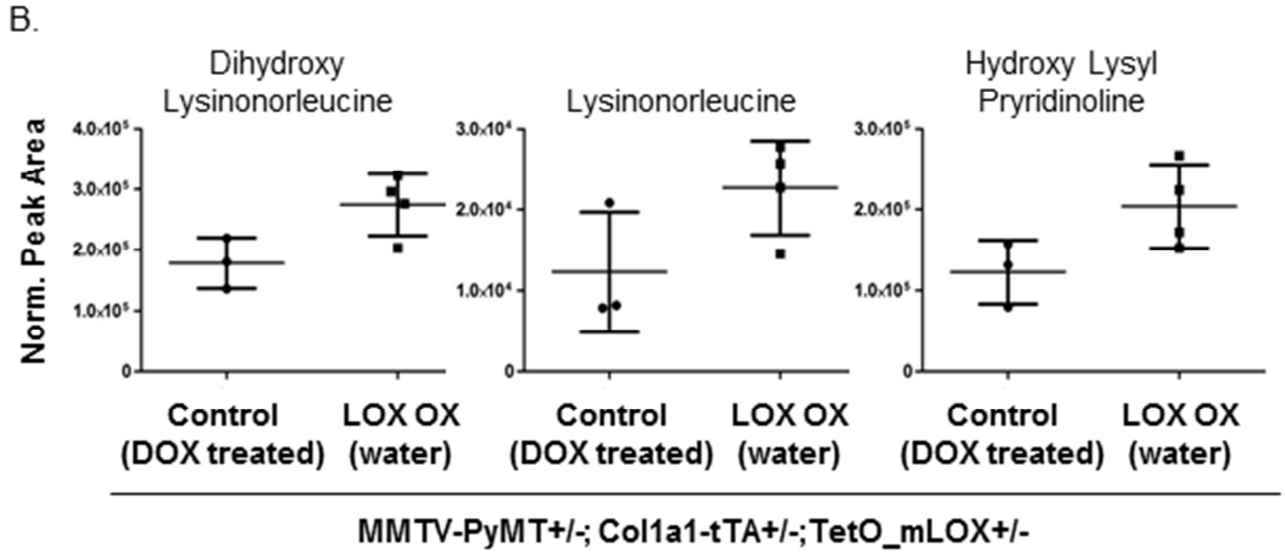
B.
Dihydroxy Lysinonorleucine
Lysinonorleucine
Hydroxy Lysyl Pryridinoline
Norm. Peak Area
Control (DOX treated)
LOX OX (water)
MMTV-PyMT+/-; Col1a1-tTA+/-;TetO_mLOX+/-

Figure 4, con't

C.

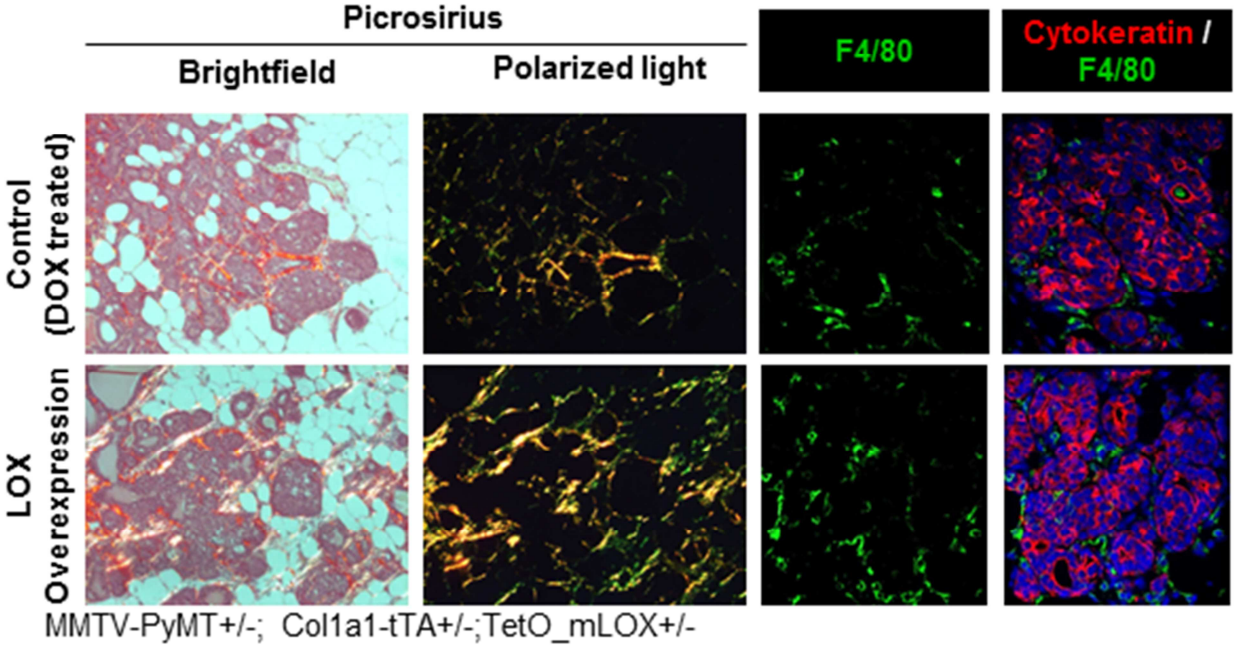

MMTV-PyMT+/-; Col1a1-tTA+/-;TetO_mLOX+/-

Figure 5

A.

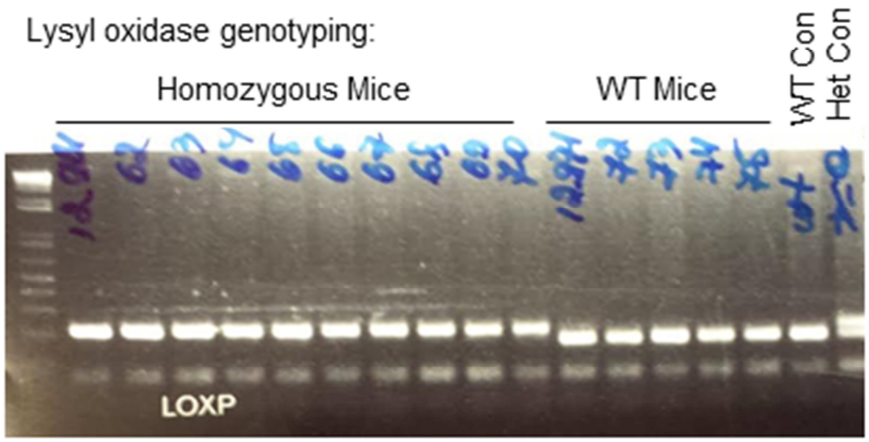
Lysyl oxidase genotyping:
Homozygous Mice
WT Mice
WT Con
Het Con
LOXP

B.

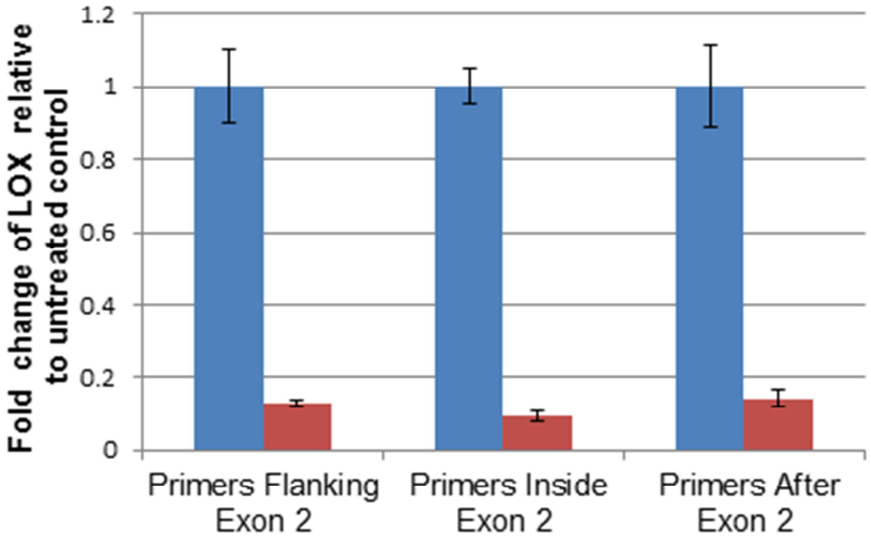
Fold change of LOX relative to untreated control
1.2
1
0.8
0.6
0.4
0.2
0
Primers Flanking Exon 2
Primers Inside Exon 2
Primers After Exon 2

Figure 6

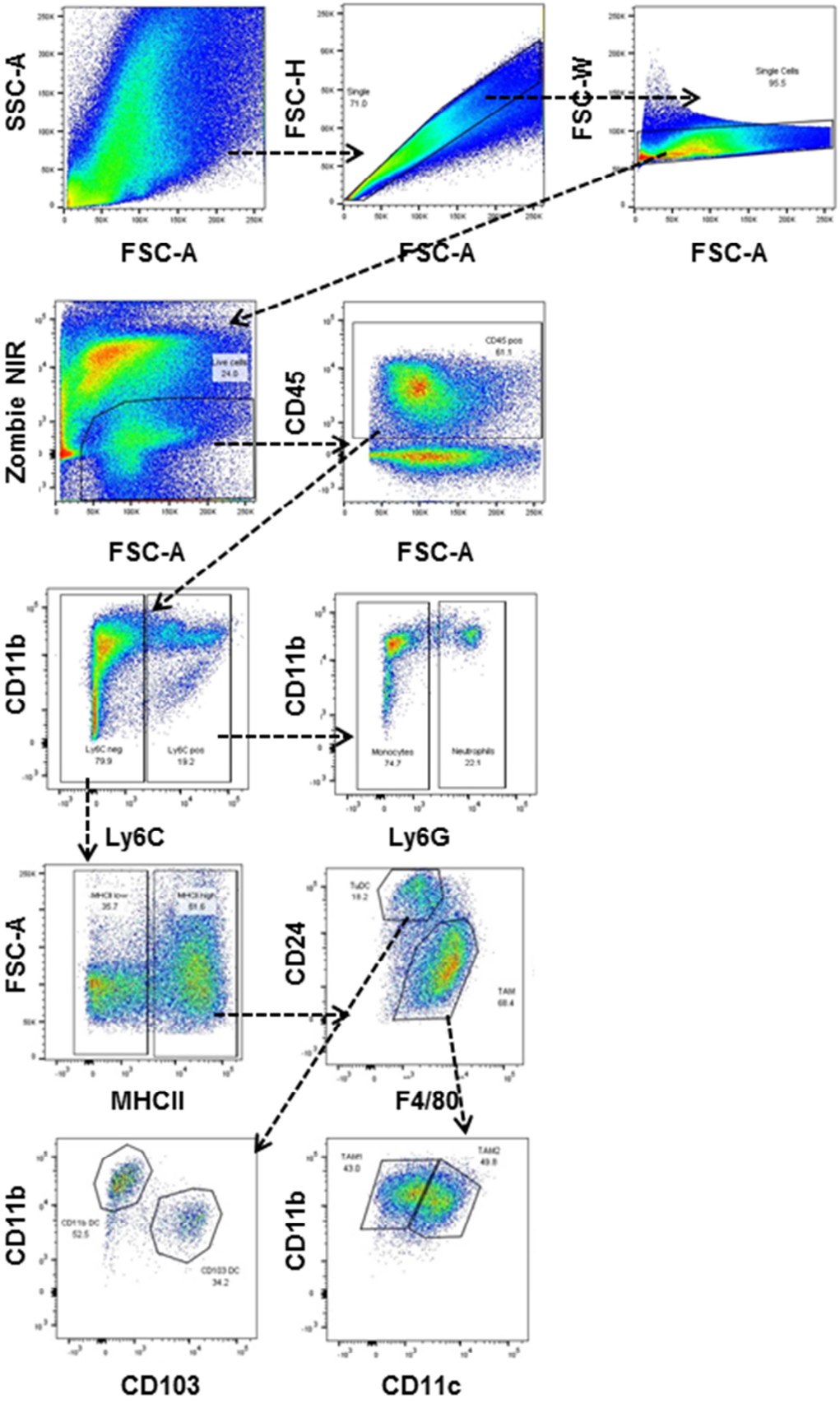
SSC-A
FSC-A
FSC-H
FSC-A
FSC-W
FSC-A
Zombie NIR
FSC-A
CD45
FSC-A
CD11b
Ly6C
CD11b
Ly6G
FSC-A
MHCII
CD24
F4/80
CD11b
CD103
CD11b
CD11c

Figure 7

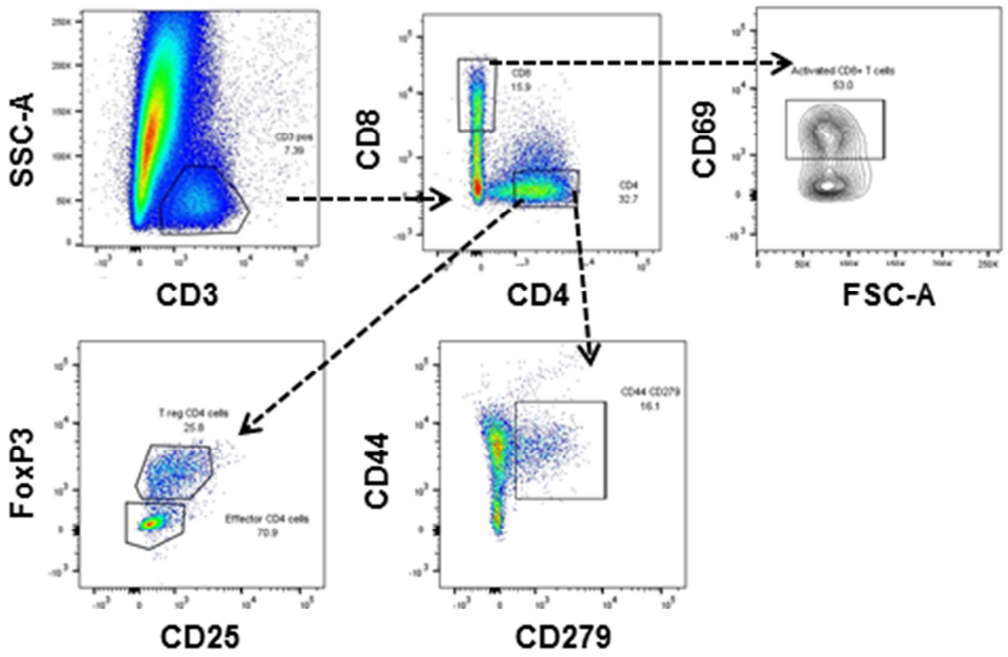
SSC-A
CD3
CD3 pos
7.39
CD8
CD4
CD8
15.9
CD4
32.7
CD69
FSC-A
Activated CD6+ T cells
53.0
FoxP3
CD25
T reg CD4 cells
25.8
Effector CD4 cells
70.9
CD44
CD279
CD44 CD279
16.1

Figure 8

A.

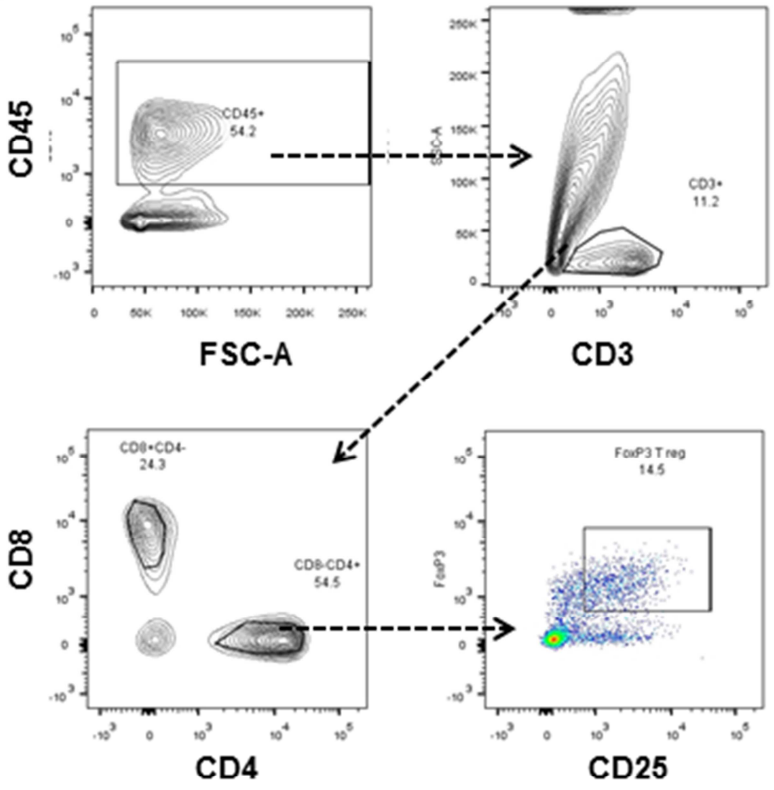
CD45
FSC-A
CD45+
54.2
CD3
CD3+
11.2
CD8
CD4
CD8+CD4-
24.3
CD8-CD4+
54.5
CD25
FoxP3 T reg
14.5

B.

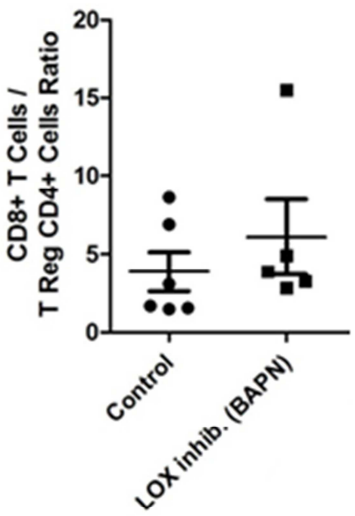
CD8+ T Cells /
T Reg CD4+ Cells Ratio
20
15
10
5
0
Control
LOX inhib. (BAPN)

Figure 9

A.

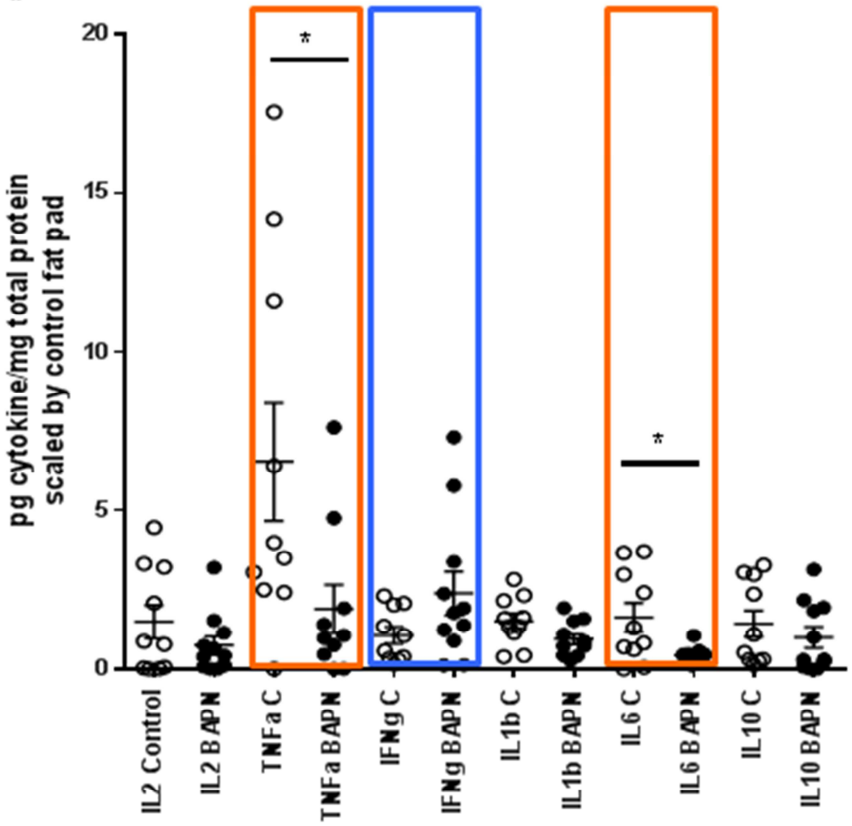
pg cytokine/mg total protein scaled by control fat pad
20
15
10
5
0
*
*
IL2 Control
IL2 BAPN
TNFa C
TNFa BAPN
IFNg C
IFNg BAPN
IL1b C
IL1b BAPN
IL6 C
IL6 BAPN
IL10 C
IL10 BAPN

B.

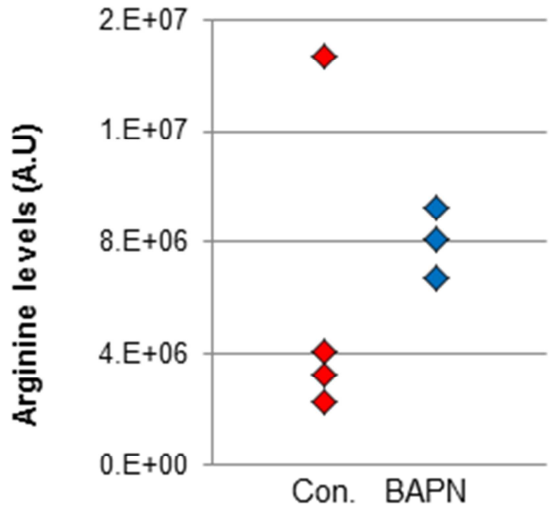
Arginine levels (A.U)
2.E+07
1.E+07
8.E+06
4.E+06
0.E+00
Con.
BAPN

Figure 10

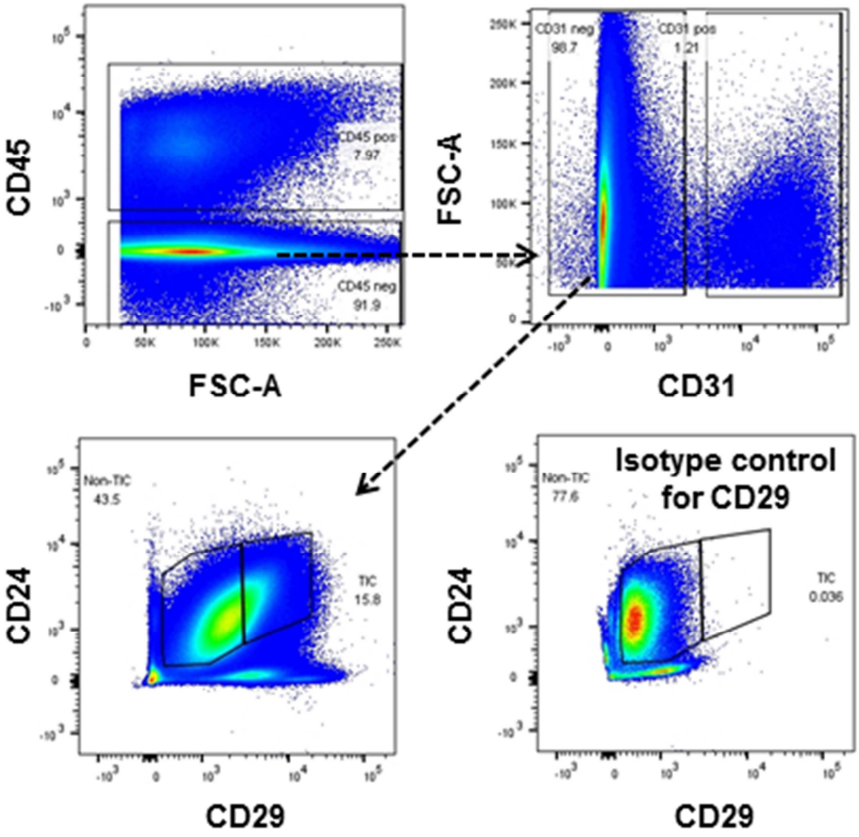
CD45
FSC-A
CD45 pos
7.97
CD45 neg
91.9
FSC-A
CD31
CD31 neg
98.7
CD31 pos
1.21
CD24
CD29
Non-TIC
43.5
TIC
15.8
Isotype control
for CD29
Non-TIC
77.6
TIC
0.036

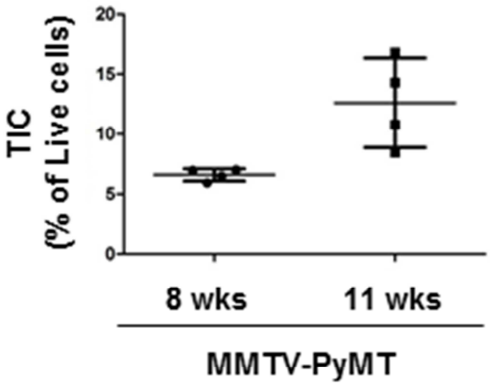
TIC
(% of Live cells)
20
15
10
5
0
8 wks
11 wks
MMTV-PyMT

Figure 11

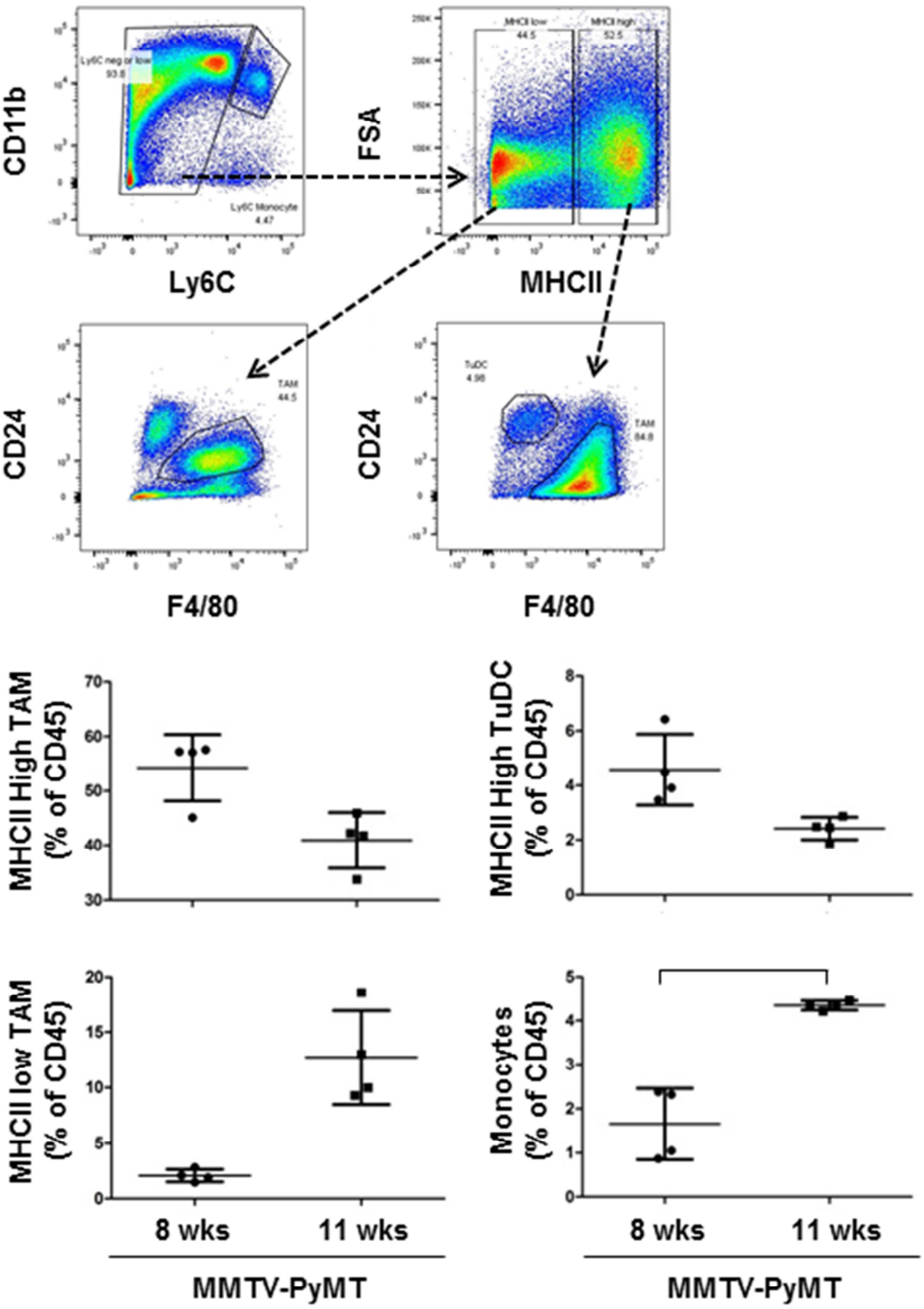
CD11b
Ly6C
FSA
MHCII
CD24
F4/80
CD24
F4/80
MHCII High TAM (% of CD45)
MHCII High TuDC (% of CD45)
MHCII low TAM (% of CD45)
Monocytes (% of CD45)
8 wks
11 wks
MMTV-PyMT
8 wks
11 wks
MMTV-PyMT

Figure 12

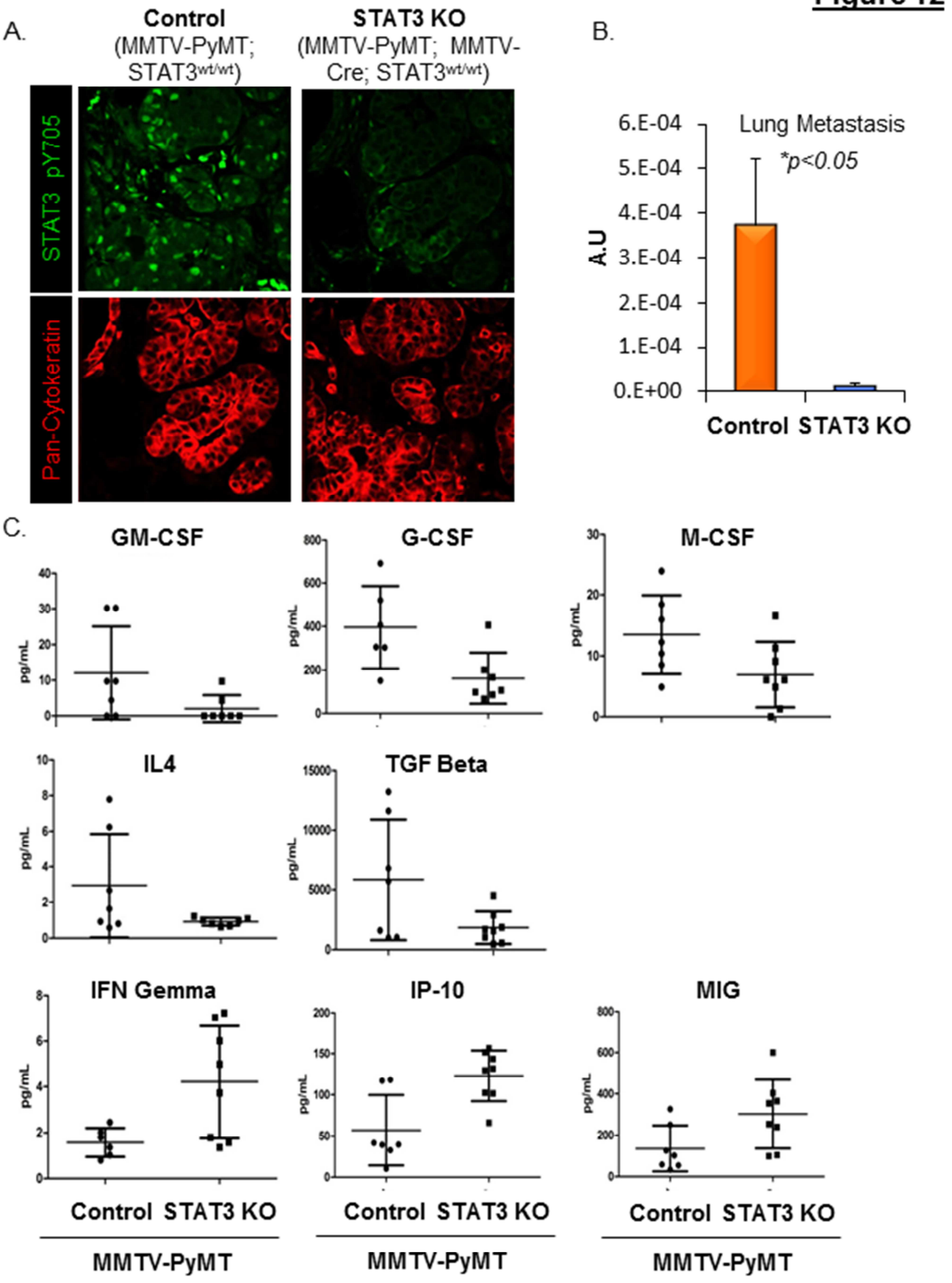
A.
Control (MMTV-PyMT; STAT3wt/wt)
STAT3 KO (MMTV-PyMT; MMTV-Cre; STAT3wt/wt)
STAT3 pY705
Pan-Cytokeratin
B.
Lung Metastasis
*p<0.05
A.U
6.E-04
5.E-04
4.E-04
3.E-04
2.E-04
1.E-04
0.E+00
Control STAT3 KO
C.
GM-CSF
G-CSF
M-CSF
IL4
TGF Beta
IFN Gemma
IP-10
MIG
pg/mL
Control STAT3 KO
MMTV-PyMT

Figure 13

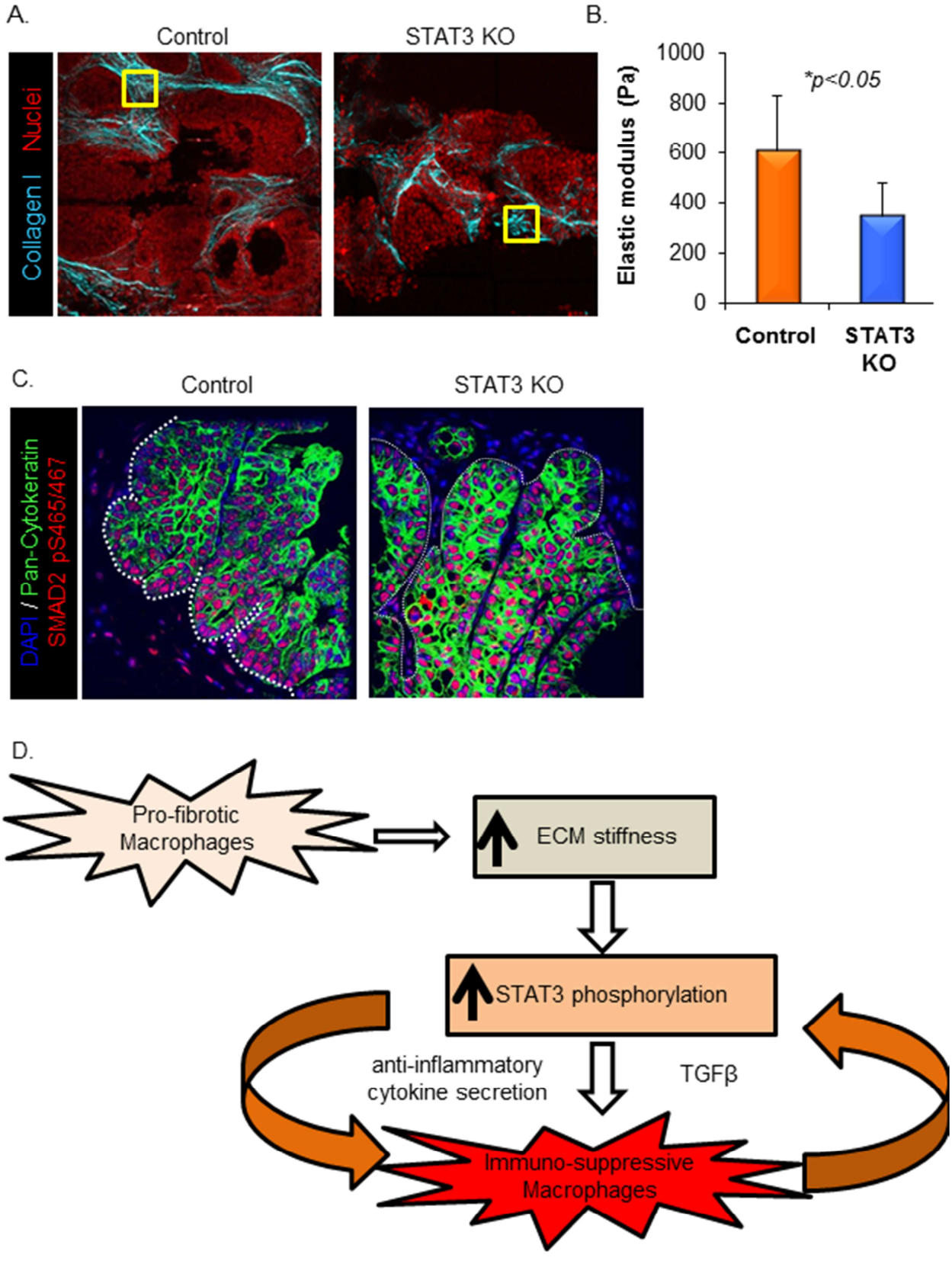
A.
Control
STAT3 KO
Collagen I
Nuclei
B.
Elastic modulus (Pa)
1000
800
600
400
200
0
*p<0.05
Control
STAT3 KO
C.
Control
STAT3 KO
DAPI / Pan-Cytokeratin
SMAD2 pS465/467
D.
Pro-fibrotic Macrophages
ECM stiffness
STAT3 phosphorylation
anti-inflammatory cytokine secretion
TGFβ
Immuno-suppressive Macrophages

Figure 14

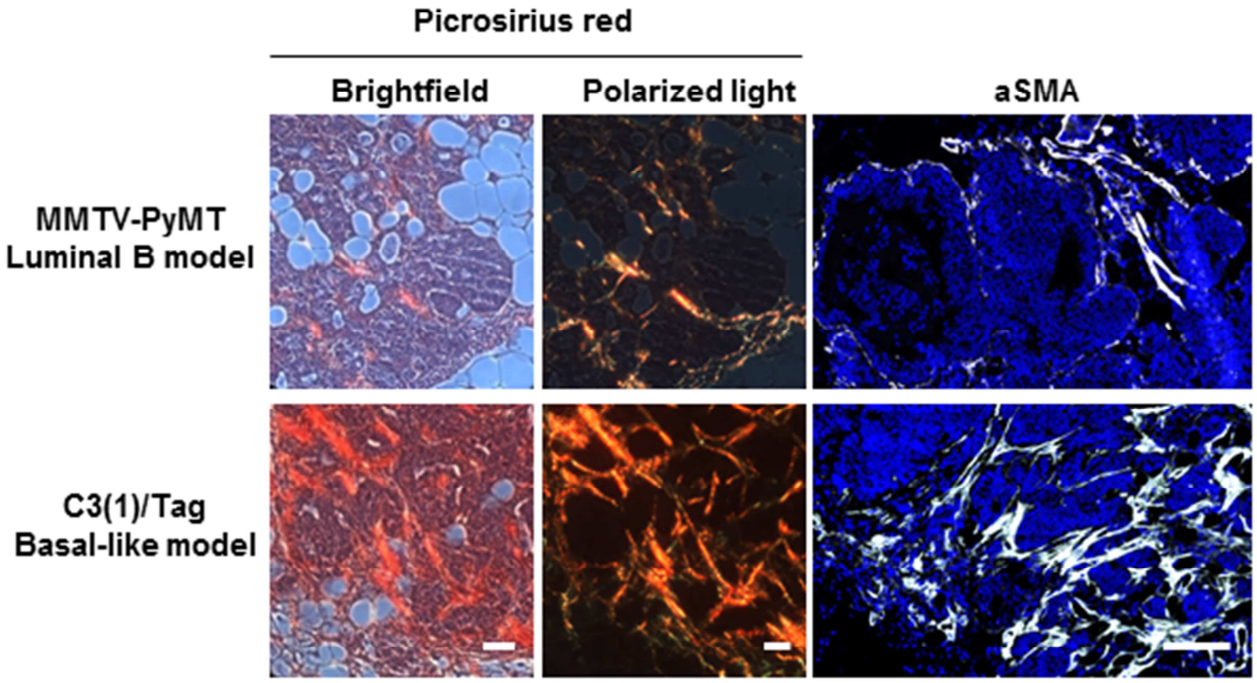
Picrosirius red
Brightfield
Polarized light
aSMA
MMTV-PyMT
Luminal B model
C3(1)/Tag
Basal-like model

Figure 15

A.

~1.5 Month
Early expression of SV40 L-Tag

2-3 Months
MIN (or DCIS)

4-5 Months
Lesions progress to carcinoma

Birth

Treatments initiated at 2 month-old mice:
- Control
- Lysyl oxidase inhibitor (BAPN)
- Low or high dose simvastatin

Mice were euthanized when they reached ~4.5 months or tumor volumes at 2/3 MG reached ~1000 mm^3

B.

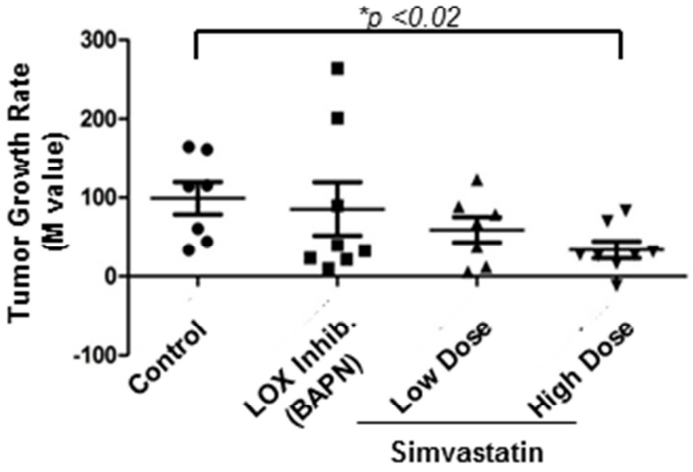

C.

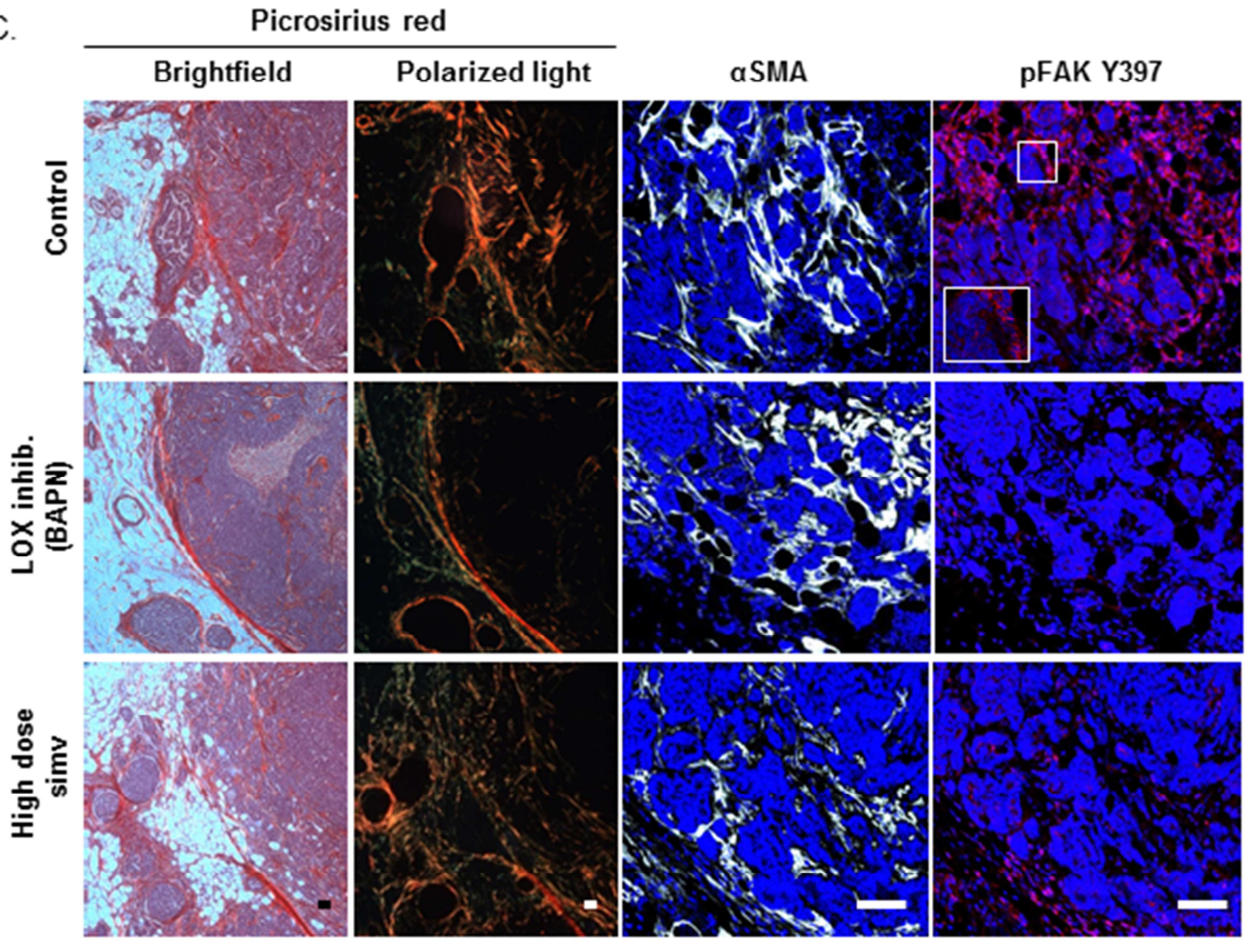

Figure 15, con't

D.

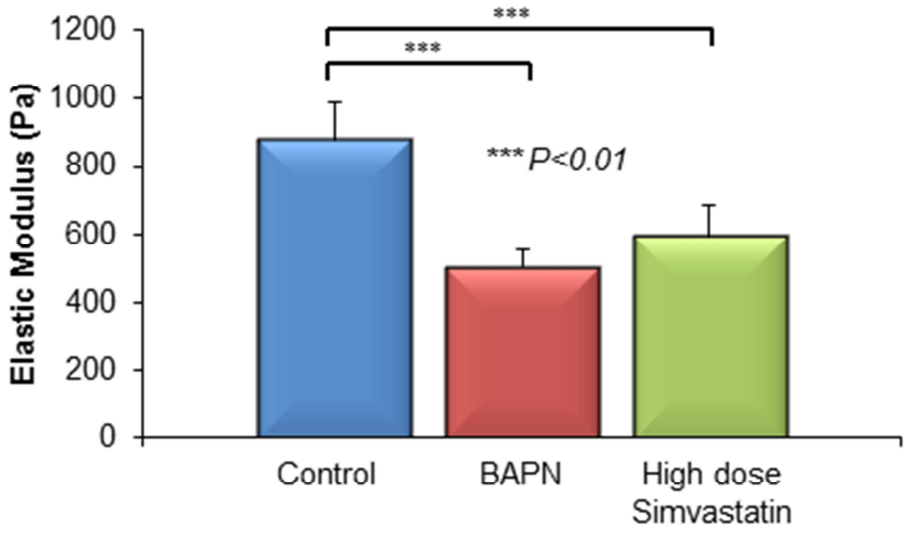

Figure 16

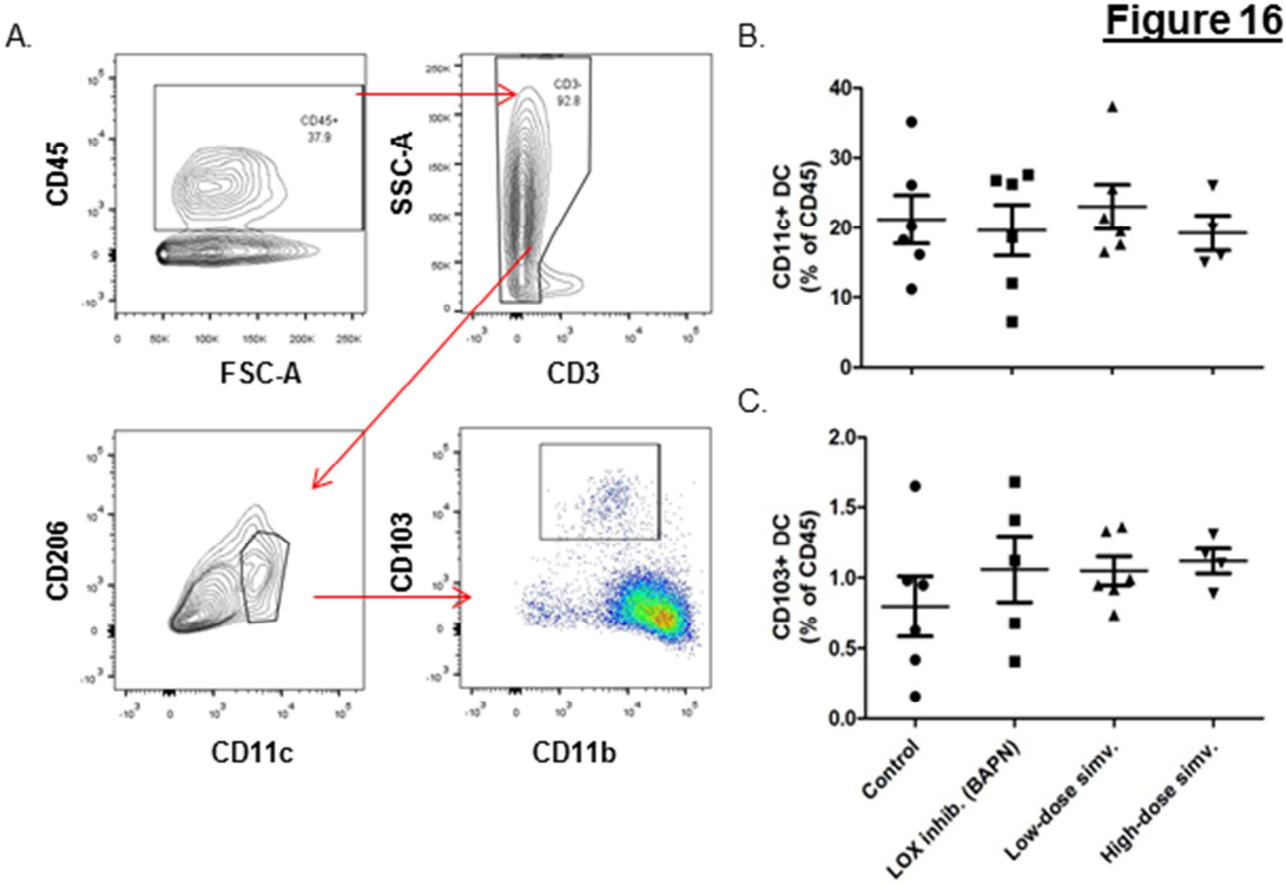
A.
CD45
FSC-A
CD45+
37.9
SSC-A
CD3
CD3-
92.8
CD206
CD11c
CD103
CD11b
B.
CD11c+ DC
(% of CD45)
40
30
20
10
0
C.
CD103+ DC
(% of CD45)
2.0
1.5
1.0
0.5
0.0
Control
LOX inhib. (BAPN)
Low-dose simv.
High-dose simv.

Professional development:

Key training and technical accomplishments:

1) I gained an extensive experience in immune cell profiling and sorting.
2) I completed a specialized AFM course at Aslyum (Santa Barbara, CA) arranged by Dr. Weaver.
3) I gained an extensive experience in performing 2 photon imaging on tissue samples and 3D collagen gels.
4) I am in the process of characterizing multiple novel transgenic models to study the role of tissue mechanics in breast cancer progression.

Key leadership roles:

1) I am a point of contact for our collaborations with: 1) Dr. Hansen (University of Colorado) on ECM proteomics and collagen crosslinking assay development; 2) Dr. Lisa Coussens (OHSU) on immune cell composition and fibrosis in mouse models of luminal B breast cancer; and 3) Dr. Matthew Krummel (UCSF) on T cell function and anti-fibrotic treatment in mouse model of basal-like/TN breast cancer.
2) I help mentor multiple graduate students.

Impact:

Nothing to Report

Products:

We are planning to submit a manuscript by the end of this calendar year or beginning of 2016.

Participants & Other Collaborating Organizations:

Name:	Luke Cassereau
Institution:	UCSF
Project Role:	Graduate Student in Dr. Weaver's lab
Researcher Identifier (e.g.ORCID ID):	Not known
Nearest person month worked:	3
Contribution to project:	Mr. Cassereau helped with the experiments involved polyacrylamide gels and AFM
Funding Support:	NRSA F31

Name:	Lisa M. Coussens
Institution:	OHSU
Project Role:	Collaborator
Researcher Identifier (e.g.ORCID ID):	Not known
Nearest person month worked:	N/A
Contribution to project:	Dr. Coussens's lab performed CSF1 Ab treatment experiment, but we did all the analyses.
Funding Support:	Not known

Name:	Kirk C. Hansen
Institution:	University of Colorado
Project Role:	Collaborator
Researcher Identifier (e.g.ORCID ID):	Not known
Nearest person month worked:	N/A
Contribution to project:	Dr. Hansen's lab measured arginine levels and collagen crosslinking in tumor tissues.
Funding Support:	NIH R33

Name:	Matthew F. Krummel
Institution:	UCSF
Project Role:	Collaborator
Researcher Identifier (e.g.ORCID ID):	Not known
Nearest person month worked:	N/A
Contribution to project:	Dr. Krummel consulted on designing immune cell panel.
Funding Support:	Not known

Special Reporting Requirements:

Nothing to Report

Appendices

Conference: CRI-CIMT-EATI-AACR - The Inaugural International Cancer Immunotherapy Conference: Translating Science into Survival

Dates: September 16 - 19, 2015

Location: Sheraton New York Times Square Hotel, New York, New York, USA

Link: AACR Conference Program

Breaking the tension: investigating a link between tissue mechanics and tumor immunity in breast cancer

Ori Maller, Luke Cassereau, Jason Northey, Brian Ruffell, Ryan Hill, Miranda L. Broz, Jennifer M. Munson, Melody A. Swartz, Kirk Hansen, Matthew F. Krummel, Lisa M. Coussens, and Valerie M. Weaver

Human breast tumors are highly fibrotic and their extracellular matrices (ECMs) are stiffer relative to benign lesions. A major contributor to tumor mechanics is fibrillar collagen-rich ECM. During tumor progression, fibrillar collagen content increases and its organization is characterized by bundles of aligned collagen fibers that are oriented perpendicular, particularly on the invasive fronts in both mouse models of breast cancer and human disease. We demonstrated that a stiffened ECM and elevated mechanosignaling (e.g. β1 integrin-focal adhesion kinase signaling axis) promoted mammary tumorigenesis, whereas reducing ECM stiffening impeded tumor formation. More recently, we established a positive correlation between the number and location of infiltrating CD45 and CD68 immune cells and ECM stiffness in human breast tumors. Infiltrating immune cells have been previously implicated in ECM remodeling associated with mammary gland development and tumorigenesis. This has led us to hypothesize that immune cells promote tumor-associated fibrosis that induces inflammatory signaling, resulting in a feed-forward loop to stimulate a pro-tumor immune response.

Using the MMTV-PyMT mouse model, we found that lysyl oxidase (LOX) inhibitor treatment — an inhibitor of collagen crosslinking — attenuated ECM stiffness and caused a shift in the cytokine milieu and increased arginine levels consistent with an anti-tumor immune response. Macrophage depletion early in PyMT tumorigenesis not only ablated metastasis, but demonstrated an anti-fibrotic role for macrophages as depicted by a decrease in fibrillar collagen and a reduction in ECM stiffness. Interestingly, we observed a striking loss of pSTAT3 and FAK signaling when mice were treated with a colony-stimulating factor 1 antagonist (anti-CSF1 antibody) early in mammary tumorigenesis. In accordance with the macrophage depletion data, STAT3 phosphorylation levels in tumor cells decreased in mammary tumors when mice were treated with a LOX inhibitor. Furthermore, the ECM adjacent to mammary tumor cells that lacked STAT3 was softer and a quantitative cytokine profiling of these tumors revealed a shift toward an anti-tumor immune response. Moreover, we demonstrated that ECM stiffness directly caused STAT3 phosphorylation in tumor cells *in vitro* by using ECM-coated polyacrylamide gels. Importantly, we also found that MMTV-PyMT primary organoids embedded in stiff collagen gels induced M0 macrophage (bone marrow derived cells previously cultured with M-CSF) differentiation and invasion.

Collectively, our data provide multiple lines of evidence to argue that macrophage infiltration promotes tumor-associated fibrosis that stimulates inflammatory signaling in tumor cells in early mammary tumorigenesis — and this feed-forward loop induces a pro-tumor immune response. These findings suggest that early treatment with an anti-fibrotic agent could mitigate immune suppression associated with late tumorigenesis and may enhance the efficacy of immunotherapy. In fact, we are now in the midst of demonstrating the effects of low-cost and well-tolerated anti-fibrotic agent on the immune component utilizing a mouse model of a basal-like breast cancer.

Acknowledgement: US DOD BCRP Postdoctoral Fellowship W81XWH-14-1-0056 (O.M.), US NIH T32 CA 108462-10 (O.M.), US NIH/NCI F31 CA183255 (L.C.), ARCS Foundation Fellowship (L.C.), US DOD BCRP W81XWH-05-1-0330 and W81XWH-13-1-0216 (V.M.W.), US NIH/NCI R01 CA192914-01 (V.M.W.), NIH/NCI R01 CA174929 (V.M.W. and C.P.), Susan G. Komen KG110560PP (V.M.W. and, E.S.H. and L.M.C.) and KG111084 (E.S.H and L.M.C.), US NIH/NCI U54CA163123 and R01 CA155331 (L.M.C.), US DOD BCRP W81XWH-10-BCRP-EOHS-EXP (L.M.C.), and US BCRF A124232 (L.M.C.)